

# A Fairness-Oriented Reinforcement Learning Approach for the Operation and Control of Shared Micromobility Services

Matteo Cederle, Luca Vittorio Piron, Marina Ceccon, Federico Chiariotti,  
Alessandro Fabris, Marco Fabris, and Gian Antonio Susto

**Abstract**—As Machine Learning grows in popularity across various fields, equity has become a key focus for the AI community. However fairness-oriented approaches are still underexplored in smart mobility. Addressing this gap, our study investigates the balance between performance optimization and algorithmic fairness in shared micromobility services providing a novel framework based on Reinforcement Learning. Exploiting Q-Learning, the proposed methodology achieves equitable outcomes in terms of the Gini index across different areas characterized by their distance from central hubs. Through vehicle rebalancing, the provided scheme maximizes operator performance while ensuring fairness principles for users, reducing iniquity by up to 80% while only increasing costs by 30% (w.r.t. applying no equity adjustment). A case study with synthetic data validates our insights and highlights the importance of fairness in urban micromobility.  
**Index Terms** - Algorithmic Fairness, Q-Learning, Reinforcement Learning, Shared Micromobility Services, Smart Mobility

## I. INTRODUCTION

With recent global advances, a growing commitment to focus on how control systems can address large societal challenges has emerged [1], [2]. In particular, over the past decade, Micromobility Sharing Systems (MSSs) have become integral to urban transit [3], providing last-mile services that complement mass transit and significantly reduce CO<sub>2</sub> emissions. This growth has driven interest in rebalancing techniques [4], which involve moving shared vehicles to areas of need. Rebalancing represents a significant cost for MSS operators, but it is necessary to consider imbalances in demand patterns and traffic limitations for the trucks that physically transport the vehicles [5].

Despite the growth of sharing services, the research community has recently raised a major concern: bikes, scooters, and other micromobility services are more available in wealthier areas, excluding poorer communities [6], due to higher densities in central areas and lower subscription rates among working-class users [7], even though the easier access to dockless MSSs [8] mitigates the problem. Clearly, unfair systems arising from a lack of attentive policies and profit-oriented management limit accessibility for disadvantaged groups, further marginalizing them and impacting their

ability to participate in essential social activities [9]. For this reason, the concern on seeking equity-based solutions has increasingly gained attention, particularly when opaque learning-based schemes are involved [10]. Specifically, the MSS equity problem is linked to spatial fairness [11], which pursues uniform resource allocation. Such a challenge, in turn, translates into balancing the trade-off between minimizing the cost of vehicle placement over densely populated or wealthier areas and adequately distributing the shared vehicles across all neighborhoods, including fairness into the optimization process. Our work investigates this trade-off in dockless MSSs, proposing a Reinforcement Learning (RL) scheme that considers the spatial fairness of the system. The main contributions of this paper are the following.

- We propose a simplified fairness-aware MSS simulator, by clustering the areas into different categories resting on the proximity to central hub stations.
- Through Monte Carlo simulations, we reveal the presence of an inherent trade-off between the MSS performance and the associated fairness level obtained by applying a parametric family of RL-based strategies.
- We analyze the trade-off between spatial fairness and overall cost in MSS operation, comparing performance-driven strategies with a new fairness-based approach. The proposed method can directly control the balance between fairness, rebalancing costs, and user disservice.
- While the abovementioned works deal with fairness in system planning, to the best of our knowledge, this is the first work on fairness in MSS operation and rebalancing.

The proposed fairness-oriented modification can reduce the iniquity of MSSs, as measured by the Gini index, by up to 80%, while only introducing a 30% additional cost (with respect to applying no equity adjustment), and even cheaper measures can still provide a significant improvement.

The remainder of this manuscript unfolds as follows. Section II covers the required preliminaries; whereas, Section III delves into the proposed approach by providing a formulation of the problem along with its RL-based solution. To support the theoretical findings, Section IV reports on a case study and examines the related fairness achievements. Lastly, conclusions and future outlooks are sketched in Section V.

*Notation:* The set of natural and real numbers are denoted by  $\mathbb{N}$  and  $\mathbb{R}$ , respectively. Given a random variable (r.v.)  $Y$ , its probability mass function is denoted by  $P[Y = y]$ , whereas  $P[Y = y \mid Z = z]$  indicates the probability mass function of  $Y$  conditioned to the value of a r.v.  $Z$ . The expected value of a r.v.  $Y$  is denoted by  $\mathbb{E}[Y]$ .

Corresponding author: M. Ceccon (marina.ceccon@phd.unipd.it).

A. Fabris is with the Max Planck Institute for Security and Privacy, 44799 Bochum Universitätsstraße 140, Germany. The remaining authors are with the Department of Information Engineering, University of Padova, 35131 Padua via Gradenigo 6/B, Italy.

This study was partially carried out within the MOST (the Italian National Center for Sustainable Mobility) and received funding from NextGenerationEU (Italian PNRR – CN0000023 - D.D. 1033 17/06/2022 - CUP C93C22002750006).

## II. SYSTEM MODEL

This section is dedicated to the preliminary notions needed for the modelling of an MSS. In addition, it reports key concepts of RL and fairness metrics finding relevance within the context of this research.

### A. Modeling of dockless MSSs

A dock-based MSS is naturally defined as a fully connected graph  $\mathcal{G} = (\mathcal{V}, \mathcal{E})$ , where a node in  $\mathcal{V}$  represents a station and  $\mathcal{E} = \mathcal{V} \times \mathcal{V}$  denotes the set of connections between each pair of stations. Each node  $i \in \mathcal{V}$  is characterized by its current occupancy, i.e., the number of vehicles present at the  $i$ -th station at time  $t$ . On the other hand, dockless systems do not have discrete pick-up and drop-off points, as users might leave the shared vehicles anywhere in the service area after their ride. However, the benefits of such an approach, and the extensive literature on docked systems, can be translated to the dockless context by considering service areas instead of stations: the set of nodes  $\mathcal{V}$  then becomes a partition of the city map, and each node represents a relatively small area, over which the number of vehicles is counted.

It is vital to observe that *accurately modeling and predicting the dynamics of such networks in their entirety is not a computationally tractable problem for large MSS services*, like the ones that we are interested in. We then focus on a stochastic model of an individual service area, considering independent Markov-Modulated Poisson Processes (MMPPs) for the arrivals and departures, which is consistent with experimental results on large sharing systems [5]. The demand rates vary according to daily, weekly, and seasonal cycles, and are affected by geographic factors as well. The vehicle occupancy of the area then follows a left-censored continuous-time Markov Birth-Death Process (MBDP), i.e., a stochastic process in which Poisson events represent either an increase or a decrease of the state by 1, and in which the rate of these events is the outcome of a Markov process with discrete time steps. The left censoring limits the state to positive values: while new arrivals are always possible (unlike in dock-based systems, in which stations have a maximum capacity), a new departure from the area is impossible if there are no vehicles to take. The transition probability from state  $m$  to state  $n$  over time  $t$  is then approximated by

$$P_{m,n}(t) \simeq \begin{cases} \sum_{l=m}^{\infty} p_{\text{Sk}}(-l; t, \lambda_a, \lambda_d), & \text{if } n = 0; \\ p_{\text{Sk}}(n - m; t, \lambda_a, \lambda_d), & \text{if } n > 0; \end{cases} \quad (1)$$

in which  $p_{\text{Sk}}(n; t, \lambda_a, \lambda_d)$  is the Skellam distribution [12], i.e., the difference of two Poisson random variables:

$$p_{\text{Sk}}(n; t, \lambda_a, \lambda_d) = e^{-t(\lambda_a + \lambda_d)} \sqrt{\lambda_a^n \lambda_d^{-n}} I_n \left( 2t \sqrt{\lambda_a \lambda_d} \right), \quad (2)$$

where  $\lambda_a$  and  $\lambda_d$  represent the arrival and departure rates, respectively, and  $I_n(\cdot)$  is the modified Bessel function of the first kind [13]. This approximation follows the work in [5], and its accuracy depends on the frequency with which areas become empty, as its accuracy is decreased by left-censoring: there can never be fewer than 0 shared vehicles in an area.

In the following, we will consider a system with  $V = |\mathcal{V}|$  service areas, which we divide in  $M$  categories according to common spatial patterns in U.S. and European cities: in general, central areas tend to see more traffic, and have an unbalanced traffic pattern with more arrivals than departures during the morning rush hours, as commuters tend to go towards commercial areas and large businesses, and more departures during the evening, while residential areas follow an inverted trend, with a lower traffic in general. Recreational areas such as parks often have yet another pattern, with more trips during the central hours of the day and no rush hour peak, and recent studies have shown [14] that identifying up to 5 different areas can provide an accurate picture of urban shared mobility. The rebalancing of each area can then be performed by adding or removing vehicles with a truck, and is usually a significant cost in the operation of an MSS.

### B. Fairness metrics in MSSs

The equity, or fairness, of MSSs has been the subject of significant attention: several studies [15], [16] have shown that the largest existing systems privilege central and wealthier areas, compounding existing inequalities in mass transit systems and urban environments more in general. However, most of the literature considers fairness for planning purposes and on a *system-level perspective*: the objective of this work is to consider fairness from the perspective of a single user, applying this metric for system rebalancing operations.

The meaning of spatial fairness from a user-level perspective is simple: what users see and are affected by is the presence of shared vehicles in their vicinity, as it determines their ability to make use of the system and move across the city. We then consider the probability that a user in a given area, i.e., often a person residing or working in that neighborhood, will be unable to find a vehicle in their immediate vicinity during rush hour. A perfectly fair system would equalize this failure probability all over the system. There is an inherent trade-off with rebalancing efficiency: enforcing fairness constraints necessitates increased movement of rebalancing vehicles to low-demand areas, which are typically more remote. This leads to reduced expected profitability compared to central, high-demand areas.

We thus consider the Gini index as a general fairness metric, following general practice in the field [15], but apply it to our user-level perspective. The Gini index is a measure of statistical dispersion of a distribution, particularly useful for assessing the equality of access to services within a population. Its values span from 0 to 1, where 0 indicates a perfectly fair system, while 1 indicates high unfairness [17]. In our context, it is defined as

$$g(x) = \frac{1}{2M^2 \bar{x}} \sum_{m=1}^M \sum_{n=1}^M |x_m - x_n|, \quad (3)$$

where  $M$  is the number of area categories,  $x_m$  denotes the probability of service failure at finding an available vehicle in a given category, and  $\bar{x}$  denotes the mean value of  $x_m$  over  $m = 1, \dots, M$ . Considering a linear combination of profit and a pure fairness metric as an objective function, instead

of a mixed metric that includes both economic incentives and system-level fairness, allows us to control the trade-off between economic and fairness concerns.

### C. Essentials of Multi-Agent Reinforcement Learning

RL is a paradigm in which one or more *agents* implicitly learn how to solve a *task*, i.e. maximizing the *cumulative rewards* obtained over time, by interacting with its *environment*. The formalization of such decision-making problem is given by the concept of Markov Decision Process (MDP) [18]. A cooperative multi-agent MDP is a tuple  $\langle \mathcal{S}, \mathcal{A}, \mathcal{P}, \mathcal{R}, \gamma \rangle$ , in which  $\mathcal{S}$  and  $\mathcal{A}$  are two finite and discrete sets, representing the state and action space respectively. In the  $N$ -agent case, each element of the action space is a vector with  $N$  elements, representing the action for each agent.  $\mathcal{P}(s, \mathbf{a}, s') = P[S_{t+1} = s' | S_t = s, A_t = \mathbf{a}]$  is the state transition probability function, which moves the environment to a new state  $s'$  at each iteration, depending on the current state  $s$  and the control actions performed by the agents, represented by vector  $\mathbf{a} = [a_1 \ \dots \ a_N]^\top$ . Finally, the reward function  $\mathcal{R}(s, \mathbf{a}, s') : \mathcal{S} \times \mathcal{A} \times \mathcal{S} \rightarrow \mathbb{R}$  is used to assign a global reward to all agents, while  $\gamma \in [0, 1)$  is the discount factor used when computing the *return*

$$G_t = \sum_{k=0}^{\infty} \gamma^k R_{t+k+1}. \quad (4)$$

The behavior of the agents is completely described by a *policy*, namely a function  $\pi : \mathcal{S} \rightarrow [0, 1]^{|\mathcal{A}|}$  that maps each state to a probability of selecting an action vector:

$$\pi(\mathbf{a}|s) = P[A_t = \mathbf{a} | S_t = s], \quad \forall \mathbf{a} \in \mathcal{A}. \quad (5)$$

We can then define the state value function  $v_\pi : \mathcal{S} \rightarrow \mathbb{R}$ , i.e., the expected return<sup>1</sup> when the agents follow policy  $\pi$ :

$$v_\pi(s) = \mathbb{E}_\pi [G_t | S_t = s]. \quad (6)$$

**Problem 1 (Multi-agent MDP):** Find an optimal policy

$$\pi^* = \arg \max_{\pi: \mathcal{S} \rightarrow \mathcal{A}} v_\pi(s), \quad \forall s \in \mathcal{S}. \quad (7)$$

The solution is the same for all states, as the optimal policy maximizes the state value function for all states [18]. If the problem is fully observable, i.e., all agents have access to the complete state, the multi-agent problem is equivalent to a centralized single-agent problem, in which a central coordinator selects the actions for all agents. Due to the curse of dimensionality and the need for perfect statistical information to find a closed-form optimal solution, it is often necessary to resort to iterative learning approaches in the large majority of practical RL problems. One of the most common single-agent algorithms is Q-Learning [19], which is guaranteed to converge to the optimal solution as long as some basic conditions are satisfied, as stated in [20].

<sup>1</sup>Notation  $\mathbb{E}_\pi$  is standard in the RL literature, see [18].

## III. REINFORCEMENT LEARNING APPROACH

We now illustrate the control approach of this study by modeling the problem as a multi-agent MDP and defining the solution. We start from the Multi-Agent Reinforcement Learning (MARL) approach for the operation and control of MSS networks, presenting the model for individual agents and the adopted reward mechanism, which stands at the core of the proposed fairness-oriented strategy. However, we emphasize that the main contribution of the paper does not lie in the RL solution itself, which follows a relatively common separability technique, but in the application of fairness principles to the control of rebalancing operations in an MSS network. The complete problem is highly complex, and may not be scalable to large networks due to the inherent computational complexity of finding the optimal policy [21].

However, our statistical model relies on an independence hypothesis: the MMPPs representing arrivals and departures in each area are assumed to be independent both from each other and from other areas' processes. Clearly, this assumption does not hold for real systems, as trips begin in an area and end in another a few minutes later, but the approximation error is surprisingly low in large-scale systems [5]: any individual area makes up such a small fraction of the total traffic that local events have negligible effects elsewhere. By properly designing the reward function, the multi-agent problem becomes a transition – and reward – independent MDP: actions from one agent have no effect on the state transitions of others, albeit the overall reward might be a nonlinear function of the individual reward. The problem can be then factorized [21] into  $V$  single-agent MDPs, which can be solved individually without losing global optimality.

The elements constituting the system state are the times of the day (morning or evening), as we consider 2 rebalancing operations per day, the category of each specific area and the number of vehicles currently available in each service area. Also, the action space for each agent is designed to be granular enough to offer meaningful choices while keeping an adequate complexity. Actions for each service area include adding or removing up to 30 vehicles, by increments of 5.

### A. Reward design and fairness considerations

The global reward function needs to take two factors into account: the first, which is the traditional objective in rebalancing applications, represents the system operator's economic interest, i.e., the profits and operational costs associated with the management of the MSS, while the second, which embodies the main novelty of our work, represents the fairness of the experience for users in different areas. In turn, the economic aspect is itself the combination of various factors. Firstly, we consider a penalty for failures, i.e., whenever a user fails to find a shared vehicle within their service area. We also include a penalty term for cluttering the sidewalks if there are too many vehicles in the same area: this is a widely discussed issue of MSSs, which may figure in contracts with city governments, as well as increasing fleet management costs. Finally, the most significant cost in managing MSSs is represented by rebalancing itself:

whenever a truck is dispatched to an area, the operator incurs a cost that is proportional to the centrality of the area. In order to consider the costs of rebalancing different areas and fairness issues between neighborhoods, we partition  $\mathcal{V}$  into  $\mathcal{V}_1, \dots, \mathcal{V}_M$ , so that  $\bigcap_{m=1}^M \mathcal{V}_m = \emptyset$  and  $\bigcup_{m=1}^M \mathcal{V}_m = \mathcal{V}$ . These  $M$  subsets represent the different areas labeled in ascending order from the most peripheral to the most central.

The global reward function then becomes

$$R_t = -\alpha \underbrace{\sum_{m=1}^M \left[ \phi(m) \sum_{i \in \mathcal{V}_m} (1 - \delta(a_{t,i})) \right]}_{=: \text{reb}_t} - \sum_{i \in \mathcal{V}} f_{t,i} \quad (8)$$

$$- \beta \sum_{m=1}^M \left[ \chi(m) \sum_{i \in \mathcal{V}_m} f_{t,i} \right] - \xi \sum_{i \in \mathcal{V}} \ell_i(s_{t,i}^v, \mu_{t,i}),$$

where  $\alpha, \beta, \xi > 0$  are constants,  $\delta$  denotes the discrete Dirac impulse and  $\chi : \{1, \dots, M\} \rightarrow [-1, 1]$  is a strictly decreasing function that satisfies  $\chi(1) = 1$ ,  $\chi(M) = -1$  and  $\chi(\lceil m - \bar{m} \rceil) = -\chi(\lfloor \bar{m} + m \rfloor)$  for all  $m \in \{1, \dots, \lceil \bar{m} - 1 \rceil\}$ , with  $\bar{m} = (1 + M)/2$ , whereas  $\phi : \{1, \dots, M\} \rightarrow [0, 1]$  is a strictly decreasing function that satisfies  $\phi(1) = 1$ . Whenever the action  $a_{t,i}$  is nonzero for the reward function in (8), the product  $\phi(m) := \alpha\phi(m)$  is subtracted from the total summation; indeed, the latter quantity can be intended as the cost of carrying out a rebalancing operation for the  $m$ -th area. Furthermore, the variable  $f_{t,i}$  represents the number of failures over the node  $i$  during the considered interval, i.e., the number of users who fail to find a shared vehicle in that area, and the product  $\tilde{\chi}(m) := \beta\chi(m)$  acts as a *temperature*, to measure the degree of importance<sup>2</sup> that is given to central areas w.r.t. the peripheral ones. Moreover, the last term of  $R_t$  accounts for the fact that the injection of further vehicles into the network should be penalized proportionally, due to the clutter and fleet maintenance issues discussed above. Such a cost is modeled proportionally to the sum of every mismatch between the current number<sup>3</sup> of vehicles  $s_{t,i}^v \in [0, \sigma_i]$  and the corresponding expected demand  $\mu_{t,i}$  (until the next rebalancing action) at each node  $i$ . To this purpose, we take the function  $\ell_i : \mathbb{N} \times \mathbb{N} \rightarrow \mathbb{R} : (z_1, z_2) \mapsto \ell_i(z_1, z_2)$  to be convex and satisfy the following properties for any couple of integers  $(z_1, z_2)$ :  $\ell_i(z_1, z_2) = \ell_i(z_2, z_1)$ ;  $\ell_i(z_1, z_2) = 0$  if and only if  $\|z_1 - z_2\| \leq \zeta_{\kappa_i}$ , for a fixed<sup>4</sup>  $\zeta_{\kappa_i} \geq 0$ , with  $\kappa_i \in \{1, \dots, M\}$  being the index for which  $i \in \mathcal{V}_{\kappa_i}$  and  $\|\cdot\|$  being any metric. Also, we assign  $\tilde{\ell}_i(\cdot, \cdot) := \xi\ell_i(\cdot, \cdot)$ .

### B. Factorized MDP representation

As we discussed above, we cluster the nodes of the MSS network into several different categories, which may fit different traffic patterns for different cities. These are distinguished by their demand patterns, as well as by the

<sup>2</sup>In general, the adjustment of the temperature plays a pivotal role in controlling the delicate balance between optimizing performance metrics [22], such as accuracy, and ensuring equity in socio-technical systems.

<sup>3</sup>The quantity  $s_{t,i}^v$  is part of the observable state  $s_{t,i}$  and it is upper-bounded by  $\sigma_i \gg \mu_{i,t}$ ,  $\forall t \geq 0$ , to render the state space finite.

<sup>4</sup>Constant  $\zeta_{\kappa_i}$  can be interpreted as a fraction of the expected arrivals  $\bar{a}_{\kappa_i}$  in all nodes  $i$  of the category  $\kappa_i$ . Henceforth, we assume that  $\zeta_{\kappa_i} = 0.5\bar{a}_{\kappa_i}$ .

overall traffic volume, which is higher for central areas and gradually decreasing for more peripheral ones. This spatial categorization is crucial for understanding how to measure a fair allocation of vehicles across the network.

We then define a single-agent sub-problem, involving a single service area, in order to divide the multi-agent MDP into more manageable components.

*Problem 2 (Single-area MDP):* Choosing

$$R_{t,i} = -\tilde{\phi}(\kappa_i)(1 - \delta(a_{t,i})) - (1 + \tilde{\chi}(\kappa_i))f_{t,i} - \tilde{\ell}_i(s_{t,i}^v, \mu_{t,i}) \quad (9)$$

as the reward function, find an optimal policy

$$\pi_i^* = \arg \max_{\pi_i : \mathcal{S}_i \rightarrow \mathcal{A}_i} v_\pi(s_i), \quad \forall s_i \in \mathcal{S}_i, \quad (10)$$

where  $s_i \in \mathcal{S}_i$  includes the state of the  $i$ -th service area, as well as the time of the day, and  $\mathcal{A}_i$  represents the actions that agent  $i$  can take.

*Proposition 1 (Separability of the MSS problem [21]):*

Given the global reward function in (8), the optimal solution to the multi-agent MDP defined by Problem 1 is given by the combination of the individual solutions to the agent problems in Problem 2. The resulting solution then enjoys the convergence properties of single-agent Q-learning.

*Proof:* The state is separable, as its transition probability of agent  $i$  is only affected by its own action  $a_{t,i}$ : two components of the state (time of day and area type) evolve deterministically, while the third (available vehicles) follows an independent process in each area. It is also trivial to prove that the global reward function in (8) is the sum of each reward function in (9). Distributed Q-Learning then converges to the optimal solution for the global problem. ■

Separating the global problem into  $V$  individual sub-problems allows for faster training: the state and action spaces become much smaller, avoiding the curse of dimensionality and granting the quick optimization of large MSSs. Also, the training can be reduced to  $M$  agents, since areas in the same class have the same statistics and thus follow the same single-agent MDP. Each agent  $m$  can be trained by exploiting the information coming from all the service areas in  $\mathcal{V}_m$ . The agents follow a linearly-annealed  $\varepsilon$ -greedy policy, which guarantees convergence for the Q-learning algorithm to the optimal solution under mild conditions (see [20]).

## IV. NUMERICAL SIMULATIONS

We now report on a case study to support the discussed theoretical findings. Next, we shall provide an extensive investigation of different strategies, to demonstrate the trade-off between performance and equity (measured by the Gini index  $g(x)$  defined in (3)) and find a viable compromise.

As already discussed in Section II-A, we have implemented four different experiments, varying the number of categories  $M$ . In particular, we have examined the cases  $M \in \mathcal{M} := \{2, 3, 4, 5\}$ . In each of these scenarios, we have considered a medium-sized micromobility sharing system as

TABLE I: Network characterization and demand hyperparameters

Scenario	Number of nodes	Skellam parameters $(\lambda_a, \lambda_d)$ for morning demand	Skellam parameters $(\lambda_a, \lambda_d)$ for evening demand
2 classes	{60, 10}	{(0.3, 2), (13.8, 7)}	{(1.5, 0.3), (10, 13.8)}
3 classes	{60, 30, 10}	{(0.3, 2), (3.3, 1.5), (13.8, 7)}	{(1.5, 0.3), (1.5, 3.3), (10, 13.8)}
4 classes	{60, 40, 20, 10}	{(0.3, 2), (0.45, 3), (9.2, 5.1), (13.8, 7)}	{(1.5, 0.3), (2.25, 0.45), (6.6, 9.2), (10, 13.8)}
5 classes	{60, 40, 30, 20, 10}	{(0.3, 2), (0.45, 3), (3.3, 1.5), (9.2, 5.1), (13.8, 7)}	{(1.5, 0.3), (2.25, 0.45), (1.5, 3.3), (6.6, 9.2), (10, 13.8)}

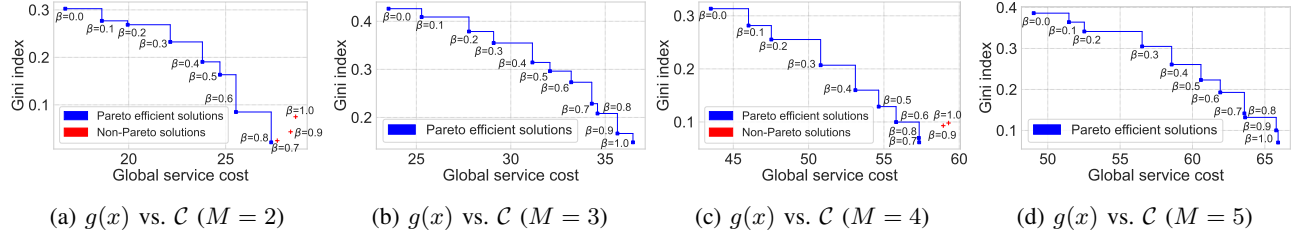


Fig. 1: Pareto fronts for the considered bi-objective optimization problem. The cost minimization and the fairness maximization objectives are represented on the x and y axes, respectively. Each mark corresponds to a different value of  $\beta$ , and the Pareto front (in blue) includes all efficient solutions. The red points correspond to Pareto-inefficient solutions.

TABLE II: Multi-agent Q-Learning hyperparameters

Learning rate	0.01	$\alpha$	20
Discount factor $\gamma$	0.9	$\xi$	0.3
Epsilon decay	$8.25 \cdot 10^{-7}$		

an example of dockless MSS. The network hyperparameters for each experiment are reported in Table I, where we recall that the categories are ordered from the most peripheral to the most central and follow realistic demand patterns [14]. For each of the experiments the training procedure starts with the service areas being subject to the demand reported in Table I. At every hour of the day  $t \in \{0, \dots, 23\}$ , the number of vehicles present in each area is updated based on the modified MBDP introduced in Section II-A. If at a certain moment a service area is unable to satisfy the demand, i.e. no vehicle is available and there is request for a departure, this is registered as a single failure for that node. The RL agents perform their control actions at 11a.m. and at 11p.m. every day through static rebalancing, as described in Section I. The training phase for each strategy is run through  $T = 10^5$  days and evaluated over  $E = 10^2$  days in the following analysis. The hyperparameters for the multi-agent Q-Learning algorithm are reported in Table II. The functions  $\phi$ ,  $\chi$ ,  $l_i$  defined in Section III-A and chosen for our experiments are assigned as follows:

- $\chi$  takes values from the array  $y_\chi := [1, .5, .4, -.5, -1]$  according to its characterization as  $M$  varies in  $\mathcal{M}$ ;
- $\phi$  takes values from the array  $y_\phi := [1, .8, .4, .3, .1]$  so that  $\phi(m) = y_\phi[k]$  if  $m, k$  are such that  $\chi(m) = y_\chi[k]$ ;
- $l_i(m) := |s_{t,i}^v - \mu_{t,i}| - \zeta_{\kappa_i}$ , for all  $m \in \{1, \dots, M\}$ .

With the above setup, we analyze the Pareto fronts of the proposed approaches, considering the trade-off between operational costs and fairness. Also, we examine the scenario  $M = 5$  in depth, by providing useful insights about the fairness and costs trends, as the fairness weighting parameter  $\beta$  in the reward function (8) varies.

### A. Pareto fronts for the proposed approach

To examine the trade-off between global service cost and fairness degree of the proposed approach we have determined the Pareto front for each of the four scenarios. Upon training and evaluating the algorithm ten times across different seeds for each value of  $\beta \in [0, 1]$ , with step-size 0.1, the average global service cost and Gini index fairness indicator have been respectively compared on the x and y axes of the Pareto diagrams in Figure 1. Specifically, we have considered as global service cost the linear combination  $\mathcal{C} := \sum_{k=1}^3 \eta_k \mathcal{C}_k$  of three sources of expenses for the service provider, where<sup>5</sup>

$$\mathcal{C}_1 := \frac{1}{E} \sum_{t=1}^E \text{reb}_t, \quad (11)$$

$$\mathcal{C}_2 := \frac{1}{E} \sum_{t=1}^E \text{fail}_t, \quad \text{with } \text{fail}_t := \sum_{i \in \mathcal{V}} \frac{f_{t,i}}{\mu_{t,i}}, \quad (12)$$

$$\mathcal{C}_3 := \frac{1}{E} \sum_{t=1}^E \text{veh}_t, \quad \text{with } \text{veh}_t := \sum_{i \in \mathcal{V}} s_{t,i}^v, \quad (13)$$

respectively denote the number of rebalancing operations, the overall service failure rate and total number of vehicles. This definition is slightly different from the reward function (8), as it considers the failure rate instead of the total number of failures and the total number of vehicles without any offsets: this can better reflect the actual costs and income of an MSS operator, while it is less effective as a reward function.

The Pareto-efficient solutions composing the frontier suggest valid choices of implementation, depending both on the desired level of fairness and the costs that the service provider is willing to bear. In Figures 1a and 1c, we can also note that, as  $\beta$  approaches 1, the solutions are not Pareto-efficient. This is expected because, as  $\beta$  increases, decisions tend to become unfair towards the most central areas, since they are almost ignored when performing rebalancing operations (see (8)). It can be shown that this phenomenon also occurs for the scenarios  $M \in \{3, 5\}$  for  $\beta > 1$ .

<sup>5</sup>Quantities  $\text{reb}_t$ ,  $f_{t,i}$ ,  $\mu_{t,i}$  and  $s_{t,i}^v$  were defined in Section III-A, while  $\eta_1 := 1$ ,  $\eta_2 := 10$ ,  $\eta_3 := 0.01$  are assumed to be given scaling factors.

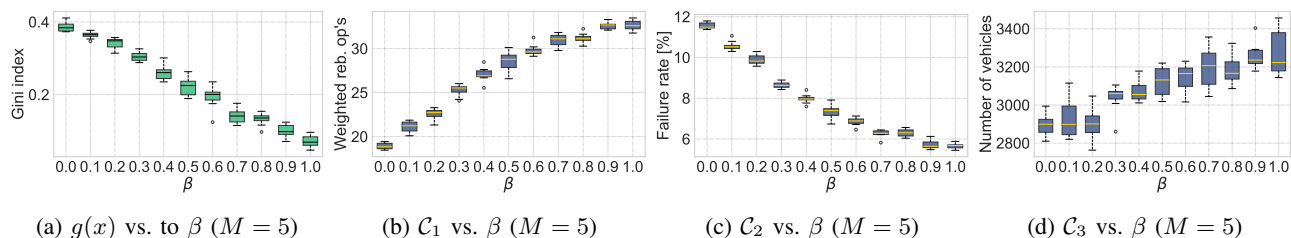


Fig. 2: Distributions over 10 Monte Carlo runs of fairness and cost-related performance metrics as a function of  $\beta$ .

Finally, we note that choosing  $M = 4$  and  $\beta = 0.7$  leads to the highest ratio (denoted by  $\rho$ ) between maximum Gini index decrease ( $-80.2\%$ ) and minimum increase for  $\mathcal{C}$  ( $+31.8\%$ ) with respect to applying no equity adjustment, i.e., setting  $\beta = 0$ .

### B. Fairness and costs trends for the five categories scenario

As said above, the scenario  $M = 5$  is explored more in detail in order to examine the distributions of both the fairness indicator and the three cost terms (11), (12), (13) encountered by the service provider as  $\beta$  varies. It can be appreciated that the monotonic trend in the Pareto front of Figure 1d is, as expected and consistent with the decreasing curve of the Gini index depicted in Figure 2a and the increasing curves of costs  $\mathcal{C}_1$  and  $\mathcal{C}_3$  respectively shown in Figures 2b, 2d. On the other hand, as illustrated in Figure 2c, the decrease of  $\mathcal{C}_2$  due to better service in disadvantaged neighborhoods is not enough to compensate for the higher costs needed to perform rebalancing operations (Figure 2b) and maintain many more vehicles in the network (Figure 2d). In this case, the highest ratio  $\rho$  is attained for  $\beta = 1$ , with Gini index decrease  $-81.6\%$  and  $\mathcal{C}$  increase  $+34.4\%$ .

## V. CONCLUSIONS AND FUTURE DIRECTIONS

This study focuses on MSS rebalancing with an emphasis on spatial fairness. A novel MARL approach resting on the network component categorization as different city areas has been designed and tested according to the selected system performance, which is based on total number of service failures, cost of all vehicles, cost of rebalancing actions and the Gini index for vehicle accessibility. Numerical results lead to balanced solutions characterized by Pareto fronts showing a sharp trade-off between overall cost and spatial fairness.

We underline that this work can be considered a seminal one as, to the best of our knowledge, we are the first to consider fairness aspects in MSS on a reinforcement learning perspective. We therefore believe that this work will lead to several extensions in the future: for example, we are planning to include time-varying demands and to consider correlations between arrival/departure processes in future formalizations.

## REFERENCES

- [1] A. Alleyne, F. Allgöwer, A. Ames *et al.*, “Control for societal-scale challenges: Road map 2030,” in *Workshop on Control for Societal-Scale Challenges*. IEEE Control Systems Society, 2023.
- [2] E. Villa, V. Breschi, and M. Tanelli, “Fair-MPC: a control-oriented framework for socially just decision-making,” *arXiv preprint arXiv:2312.05554*, 2023.
- [3] L. Cheng, Z. Mi, D. Coffman *et al.*, “The role of bike sharing in promoting transport resilience,” *Networks and Spatial Economics*, pp. 1–19, 2021.
- [4] M. Dell’Amico, E. Hadjicostantinou, M. Iori, and S. Novellani, “The bike sharing rebalancing problem: Mathematical formulations and benchmark instances,” *Omega*, vol. 45, pp. 7–19, 2014.
- [5] F. Chiariotti, C. Pielli, A. Zanella, and M. Zorzi, “A bike-sharing optimization framework combining dynamic rebalancing and user incentives,” *ACM Trans. Autonomous and Adaptive Systems (TAAS)*, vol. 14, no. 3, pp. 1–30, 2020.
- [6] X. Guan, D. van Lierop, Z. An, E. Heinen, and D. Ettema, “Shared micro-mobility and transport equity: A case study of three European countries,” *Cities*, vol. 153, p. 105298, 2024.
- [7] K. Hosford and M. Winters, “Who are public bicycle share programs serving? an evaluation of the equity of spatial access to bicycle share service areas in Canadian cities,” *Transportation Research Record*, vol. 2672, no. 36, pp. 42–50, 2018.
- [8] S. Meng and A. Brown, “Docked vs. dockless equity: Comparing three micromobility service geographies,” *J. Transport Geography*, vol. 96, p. 103185, 2021.
- [9] Z. Chen, D. Van Lierop, and D. Ettema, “Dockless bike-sharing systems: what are the implications?” *Transport Reviews*, vol. 40, no. 3, pp. 333–353, 2020.
- [10] S. Caton and C. Haas, “Fairness in machine learning: A survey,” *ACM Computing Surveys*, vol. 56, no. 7, pp. 1–38, 2024.
- [11] E. Soja, “The city and spatial justice,” *Justice Spatiale/Spatial Justice*, vol. 1, no. 1, pp. 1–5, 2009.
- [12] J. G. Skellam, “The frequency distribution of the difference between two Poisson variates belonging to different populations,” *J. the Royal Statistical Society Series A: Statistics in Society*, vol. 109, no. 3, pp. 296–296, 1946.
- [13] M. Abramowitz and I. A. Stegun, *Handbook of mathematical functions with formulas, graphs, and mathematical tables*. US Government printing office, 1968, vol. 55.
- [14] N. A. Weinreich, D. B. van Diepen, F. Chiariotti, and C. Biscio, “Automatic bike sharing system planning from urban environment features,” *Transportmetrica B: Transport Dynamics*, vol. 11, no. 1, p. 2226347, 2023.
- [15] D. Duran-Rodas, D. Villeneuve, F. C. Pereira, and G. Wulforst, “How fair is the allocation of bike-sharing infrastructure? framework for a qualitative and quantitative spatial fairness assessment,” *Transportation Research Part A: Policy and Practice*, vol. 140, pp. 299–319, 2020.
- [16] L. Su, X. Yan, and X. Zhao, “Spatial equity of micromobility systems: A comparison of shared e-scooters and docked bikeshare in Washington DC,” *Transport Policy*, vol. 145, pp. 25–36, 2024.
- [17] C. Gini, “Measurement of inequality of incomes,” *The Economic Journal*, vol. 31, no. 121, pp. 124–125, 1921.
- [18] R. S. Sutton and A. G. Barto, *Reinforcement learning: An introduction*. MIT press, 2018.
- [19] C. J. C. H. Watkins, “Learning from delayed rewards,” Ph.D. dissertation, King’s College, Cambridge (UK), 1989.
- [20] C. Szepesvári, “The asymptotic convergence-rate of q-learning,” in *Advances in Neural Information Processing Systems*, vol. 10, 1997.
- [21] R. Becker, S. Zilberstein, V. Lesser, and C. V. Goldman, “Solving transition independent decentralized Markov decision processes,” *J. Artificial Intelligence Research*, vol. 22, pp. 423–455, 2004.
- [22] S. A. Friedler, C. Scheidegger, S. Venkatasubramanian *et al.*, “A comparative study of fairness-enhancing interventions in machine learning,” in *Conf. Fairness, Accountability, and Transparency (FAT\*)*. ACM, 2019, pp. 329–338.